https://doi.org/10.2352/EI.2025.37.15.AVM-116

Flex-PLACE: Flexible Robot Base Placement for Industrial Inspection

Vanessa Staderini[1] **, *Tobias Glück***[1] **, *Andreas Kugi***[1,2]
[1] ***AIT Austrian Institute of Technology GmbH, Vienna, Austria***
[2] ***Automation and Control Institute (ACIN), TU Wien, Vienna, Austria***

Abstract

Automatic visual quality inspection is a cornerstone of modern manufacturing, leveraging advancements in computer vision and robotics to enhance speed and efficiency. While numerous inspection planning methodologies exist, they often neglect the critical challenge of designing the inspection cell—specifically, determining the optimal placement of the robot relative to the inspected objects. This placement is pivotal for maximizing inspection performance and minimizing the inspection time.

In this work, we present a flexible framework to determine the robot base placement via an optimization routine to facilitate the inspection of diverse objects. This eliminates the need to reprogram the inspection cell whenever the object changes, significantly simplifying and streamlining the process. Extensive simulations validate the effectiveness of our method, demonstrating significant improvements in achieving high coverage and reducing the time compared to a brute force approach.

Introduction

As the manufacturing industry advances, robotic systems are increasingly employed to enhance production speed and efficiency. This shift is driven by growing product diversity and the demand for high-quality standards, making rigorous quality assurance essential at various production stages. While manual inspection is often used, it is time-consuming and prone to errors caused by human fatigue and inattention. The rapid development of 3D sensor technology and robotics has enabled automatic inline inspection, leading to a rising demand for flexible, automated production systems. However, automating visual inspection poses challenges due to complex 3D geometries and diverse defect types.

Effective inspection planning must address the coverage path planning problem, encompassing two key sub-problems: the viewpoint planning problem (VPP), which identifies optimal camera poses for object inspection, and the path planning problem (PPP), which defines a time-optimal, collision-free trajectory for the robot. Typically, optimal viewpoints are determined without considering kinematic constraints, leaving feasibility checks for robotic configurations as an afterthought. However, ignoring these constraints can compromise inspection coverage and effectiveness.

Moreover, current inspection planning methodologies often neglect the design of the inspection cell—specifically, the optimal placement of the robot relative to the inspected objects. This oversight significantly impacts inspection performance and increases the time required for the inspection. Addressing this issue is crucial for improving flexibility and efficiency in visual inspection tasks.

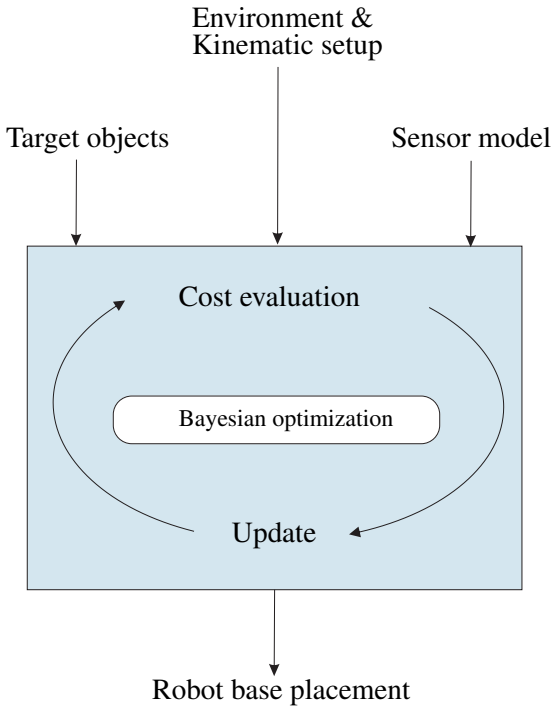

Figure 1: Framework for inspection planning: Given some external specifications, i.e., the model of target objects, specifications about the industrial scenario and the sensor model, a Bayesian optimizer is involved to compute the most suitable robot base placement.

In this work, we propose a flexible methodology to determine the optimal pose of the robot base for inspected objects with varying geometries and sizes. Our algorithm leverages black-box optimization to integrate computer vision and robotics requirements, systematically accounting for the sensor model, environment, and robot kinematic constraints. A key advantage of our approach is its independence from object geometry and size.

Extensive simulations validate the effectiveness of our algorithm, demonstrating improved performance in achieving high coverage and reducing inspection time.

The paper is organized as follows: Section 2 reviews the state of the art in robot base placement (RBP) planning. Section 3 introduces our methodology and formulation. Section 4 presents and discusses the results, while Section 5 concludes the paper.

Related works

Several studies have addressed the optimization of robot placement by considering manipulability metrics, see [1, 2, 3]. For example, [4] optimizes manipulator placement by maximizing dexterity, defined as the number of orientations the end-effector (EE) can achieve at a given point. This differs from our approach, as we prioritize ensuring the robot can meet the position and orientation requirements of the end-effector while avoiding self-occlusions and accounting for collisions. Other works focus on optimizing the robot placement to minimize a cost function related to the task of interest. The authors of [5] propose optimizing the relative robot/task position to minimize cycle time for task execution. However, no collision avoidance is considered, a key aspect in real applications. The work [6] introduces a comprehensive framework to minimize cycle time, considering task visit order, inverse kinematics (IK) solutions, and robot placement in terms of position and orientation. However, their approach is computationally prohibitive for our scenarios, which involve at least double the number of inspection points compared to the 12 task points handled in their study.

In [7], the authors optimize robot placement across multiple workpieces to enhance flexibility. This approach improves adaptability, but comes with significant computational costs. In contrast, our work focuses on determining a robot placement that remains effective when inspecting objects of varying dimensions and geometries. This is achieved by optimizing the robot's location and considering inspection poses for multiple objects.

An optimization procedure for robot base placement in industrial pick-and-place sequences is proposed in [8]. The method employs a point-to-point trajectory planner that evaluates placements while considering robot kinematic limits, collisions, and task constraints. The authors investigated goals such as cycle-time optimality, time-energy optimality, and throughput adaptivity, using Bayesian optimization to achieve efficient results. However, their approach is tailored to pick-and-place tasks with predefined task sequences, limiting its suitability to scenarios involving diverse object geometries or inspection tasks.

In our work, the primary goal is to achieve full coverage of the inspected object. For this reason, we propose adopting Bayesian optimization to maximize the coverage while reducing the inspection time. Unlike [8, 9], we do not perform cycle time optimization considering task sequences, as it would be computationally expensive and less relevant to our objectives. Instead, we focus on identifying a robot placement suitable for various objects and their associated inspection poses, ensuring flexibility and adaptability.

Method

In this work, we propose a method to optimize the placement of the robot base, which is essential for designing a flexible robotic cell for inspection tasks. The focus lies on a spatially constrained robotic cell in a restricted environment. A 6-degree-of-freedom robotic arm, equipped with a camera mounted at its end-effector, performs visual inspection tasks for objects of varying geometries and sizes. The inspection cell must enable flexible robot positioning to inspect different objects without relocation. An offline inspection plan is essential to ensure efficient online inspection, providing full coverage in the shortest possible time.

The main contributions of this work are as follows:

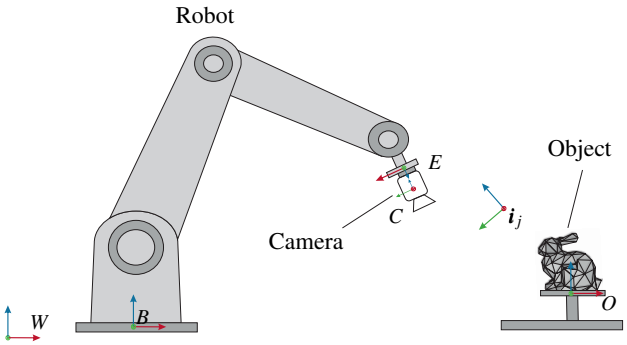

Figure 2: Illustration of a robot inspection setup: The robot aligns the camera defined by frame C with the inspection pose $\boldsymbol{i}_j$ to inspect the object with frame O. The base and end-effector frames of the robot are B and E, respectively. The global reference is the world frame W.

- We propose a novel methodology to optimize robot base placement tailored to inspection tasks in constrained environments.
- We design a cost function that integrates inspection pose feasibility, inverse kinematic solution availability, and spatial compactness, aiming to maximize coverage while minimizing inspection time.
- The proposed method ensures adaptability to objects of varying geometries and sizes, eliminating the need for robot base relocation during inspection.

Kinematic planning problem

Given a robot with n degrees of freedom, the forward kinematics of the end-effector frame E with respect to the robot base frame B is given by

$$\begin{bmatrix} \mathbf{p}_B^E \\ \mathbf{o}_B^E \end{bmatrix} = \mathbf{h}(\mathbf{q}), \tag{1}$$

where the joint configuration $\mathbf{q}^\top = \begin{bmatrix} q_1 & \cdots & q_n \end{bmatrix}$ contains the generalized coordinates of the robot. The pose (1) consists of the Cartesian position vector $\mathbf{p}^\top = \begin{bmatrix} x & y & z \end{bmatrix}$, and the orientation is expressed as unit quaternion $\mathbf{o}^\top = \begin{bmatrix} \eta & \boldsymbol{\varepsilon}^\top \end{bmatrix}$, with scalar part η and vector part $\boldsymbol{\varepsilon}$. Similarly, the pose (1) can also be expressed as a homogeneous transformation

$$\mathbf{H}_B^E = \begin{bmatrix} \mathbf{R}_B^E & \mathbf{p}_B^E \\ \mathbf{0} & 1 \end{bmatrix}, \tag{2}$$

with rotation matrix $\mathbf{R}_B^E \in SO(3)$ associated with the orientation $\mathbf{o}_B^E$.

The inspection task requires aligning the camera frame C with the inspection pose $\boldsymbol{i}_j$ to collect relevant data for the object under inspection. A pose is considered feasible if it satisfies the following conditions:

- The joint coordinates $\mathbf{q}_j[l]$, for $l = \{1, \ldots, n\}$, are within the joint limits, i.e., $\mathbf{q}_j[l] \in [\underline{q}_l, \overline{q}_l]$.
- The robot avoids collisions with itself and the environment.
- The line of sight between the sensor and the object remains unobstructed.

Therefore, choosing an optimal robot base placement is critical to reducing the number of unfeasible inspection poses and improving the inspection's performance.

Problem Formulation

The framework we propose begins by computing N inspection poses using the Poisson Surface Sampling method [10] for objects of varying shapes and sizes. The objective is to determine the robot base pose $\mathbf{H}_W^B$ within predefined bounds in the operating environment $\mathscr{W}$, where $\mathscr{W}$ includes static obstacles $\mathscr{C}$. The base orientation is neglected as we assume the rotational flexibility of the first two joints.

An inspection pose $\mathbf{i}^f \in I^f$ is feasible if at least one feasible inverse kinematic solution exists. Feasible inverse kinematic solutions $\mathbf{q}^f \in Q^f$ ensure no collisions and an unobstructed line of sight.

To evaluate candidate robot placements, we define a cost function that balances three key terms:

1. **Inspection Pose Feasibility:** The number of feasible inspection poses ($|I^f|$) normalized by the total number of inspection poses (N) is defined as:

$$F_1 = \frac{|I^f|}{N}. \tag{3}$$

2. **Pose Distribution Sparsity:** The average distance between feasible inspection poses, normalized by the maximum distance between all inspection poses $d^{\max}(I)$ is given by

$$F_2 = \frac{\bar{d}^f}{d^{\max}(I)}. \tag{4}$$

Here, $\bar{d}^f$ is the average Euclidean distance (d) between all elements of the set I^f and is defined as

$$\bar{d}^f = \frac{1}{|I^f|(|I^f|-1)} \sum_{\substack{k,j \in I^f \\ k \neq j}} d(\mathbf{i}_k^f, \mathbf{i}_j^f). \tag{5}$$

3. **Inverse Kinematic Solution Availability:** The number of feasible inverse kinematic solutions ($|Q_k^f|$) for the k-th end-effector's pose $\mathbf{i}_k$ normalized by the total number of inverse kinematic solutions (M)

$$F_3 = \frac{|Q_k^f|}{M}. \tag{6}$$

The objective of these three terms is to: (i) maximize the number of feasible inspection poses, (ii) ensure the sparsity of feasible poses to enable coverage of different areas of the object, and (iii) increase the number of feasible inverse kinematic solutions to accelerate the inspection process.

The overall cost function is defined as:

$$F(\mathbf{H}_W^B) = F_1 + aF_2 + bF_3, \tag{7}$$

where $a > 0$ and $b > 0$ are weighting parameters that adjust the trade-off between feasibility, sparsity and, robustnes. For robots with an infinite number of solutions, (7) can be adapted by setting $b = 0$. This general formulation enables an optimizer to determine the optimal robot placement as:

$$\mathbf{H}_W^{B\,*} = \arg \max_{\mathbf{H}_W^B \in \mathscr{C}^{free}} F\left(\mathbf{H}_W^B\right), \tag{8}$$

where $\mathscr{C}^{free} = \mathscr{W} \setminus \mathscr{C}$ is the free space within the operating environment $\mathscr{W}$ without colliding with an obstacle in $\mathscr{C}$.

We employ Bayesian optimization [11, 12] to solve this optimization problem numerically. This black-box optimization method is particularly efficient for high-cost evaluations as it balances exploration and exploitation. Additionally, it uses an acquisition function to guide the selection of subsequent evaluation points, minimizing extensive search.

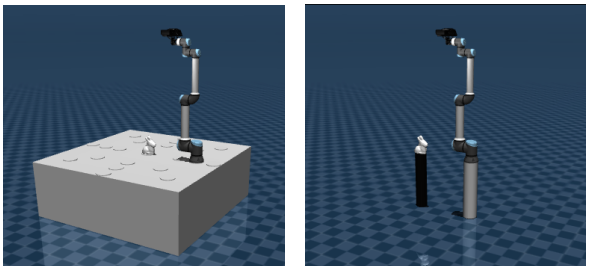

(a) Scenario 1 (b) Scenario 2

Figure 3: Testing scenarios.

Experiments

We conducted several simulation tests to validate our approach using the collaborative robot UR10e[1] universal robot. This 6-DOF robot allows for up to eight distinct joint configurations ($M = 8$) [13] for a given end-effector pose. Our novel algorithm was evaluated in simulation across two scenarios, as illustrated in Figure 3.

- Scenario 1: The robot and the inspected object are placed on the same block.
- Scenario 2: The robot and the inspected object are on two different supports and are not connected.

The goal is to demonstrate that our algorithm allows us to determine the best robot base placements (RBP) and also helps to determine the most suitable cell design (e.g., one big block or two distinct columns). For this reason, the two scenarios were compared starting from the same inspection poses. These were generated for objects with diverse geometries and sizes, as shown in Figure 4. These objects included a convex rabbit, a cup, and a Lego object [14]. This selection was designed to test the algorithm's flexibility and enhance its performance in achieving high final coverage. We generated 15 inspection poses for each object, resulting in a set of 45 diverse inspection poses used to determine the robot base position that maximizes the cost function (7). We discretized the locations where the robot can be placed in 160 locations: these were determined as 20 different positions in the XY plane where the robot can be placed at a height between 0 and 0.7 m. We spaced the different heights at 1 cm difference.

[1] `https://www.universal-robots.com/products/ur10-robot/` (Accessed January 7, 2025)

(a) Rabbit (b) Cup (c) Lego

Figure 4: 3D meshes of the objects used in the experiments to determine the best robot base placement.

The 20 locations are visualized in Subfigure (a) of Figure 3 as circular shapes. The orientation of the robot's base was neglected, as the first two joints of the UR10e robot can freely rotate between 0° and 360°. In our application, we want to balance the *inspection pose feasibility*, the *pose distribution sparsity*, and the *inverse kinematic solution availability* according to (7). For this reason we set the tuning parameters to $a = b = 1$.

In order to prove the advantage of using our method, we first determined the best robot placement by evaluating all the possible configurations (i.e., 160 combinations). The position $(x, y, z) = (-0.75, 0, 0.4)$ provides the maximum score for Scenario 1 corresponding to $F = 1.42$. The combination $(x, y, z) = (-0.5, 0, 0)$ provides the maximum score for Scenario 2 corresponding to $F = 1.52$. Then, we adopted our algorithm to find the best robot placement, as shown in Figure 5. We set the number of exploration and exploitation to 20 for a total of 40 iterations in the case of Scenario 1, and 40 iterations of exploration and exploitation in the case of Scenario 2. The proposed approach converges to the true maximum in both scenarios. Moreover, the method identifies the same robot base position as when the brute force approach was adopted, but in a time that was three times faster.

Figure 6 illustrates the interpolated objective value distribution for fixed z values in two scenarios. Subfigure (a) represents Scenario 1 with $z = 0.4$, while Subfigure (b) depicts Scenario 2 with $z = 0$. The surfaces are obtained by interpolating discrete data points (i.e., the objective values), and the color gradient of the heatmap reflects the objective value distribution, where darker shades indicate lower values and lighter shades represent higher values, with the peak highlighted in yellow. The maximum value of the score, computed from the raw data, is marked with a red star. Additionally, the green, blue, and orange circles denote the maximum values for inspection pose feasibility ($F = F_1$ in (8)), pose distribution sparsity ($F = F_2$ in (8)), and inverse kinematic solution availability ($F = F_3$ in (8)), respectively, with each value normalized between 0 and 1. It is important to note that the interpolation process smooths the discrete data points to create a continuous surface. As a result, the actual maximum scores from the raw data (1.42 for Scenario 1 and 1.52 for Scenario 2) are not visualized precisely on the plots. Instead, the red stars indicate their locations based on the raw data, helping to highlight the true peaks despite potential smoothing effects in the visualization.

Once the robot placement was determined, an inspection plan was derived for three new objects, see Figure 7: a parallelepiped, an industrial component referred to as gear[2], and a dog. The performance in terms of achieved coverage and required inspection time were compared to the case in which the robot base placement was not optimized, and the results are summarized in Table 1. We derived an inspection plan for the three objects and

[2]`https://owncloud.fraunhofer.de/index.php/s/H8jV9rwGN84knzP` (Accessed January 7, 2025)

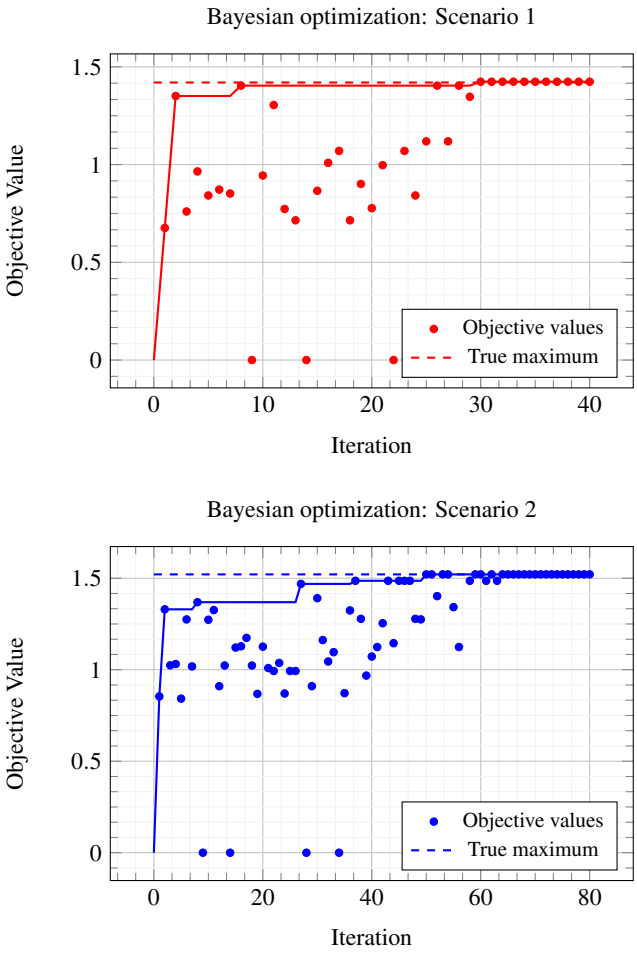

Figure 5: Convergence plots for Scenario 1 (in red) and Scenario 2 (in blue): The true maximum was found evaluating all the possible robot placement locations.

the two scenarios starting from a set of 50 inspection poses. This represents a good initial value for various objects to obtain high coverage while keeping the number of optimal inspection poses low. The performance of our planning is reported in terms of coverage (%), the number of feasible inspection poses (#FIPs) considered as the set of poses from which to extract the optimal inspection poses solving the set coverage problem, and the average transition time to go from one inspection pose to another one in seconds (s). As expected, the number of feasible inspection poses and achieved coverage is higher when the robot base placement is optimized (Position 1 and Position 3 for Scenario 1 and 2, respectively). Position 2 was chosen as the location with the lowest score during the brute force approach. Moreover, the coverage and the number of feasible inspection poses are higher when the object and the robot are placed on two individual columns (Scenario 2). This has the consequence of keeping the transition time small despite having a higher sparsity of the pose distribution. Finally, our experiments prove the suitability of using two separated columns instead of placing both object and robot on the same block. This increases the number of feasible inspection poses by 5% points and improves the coverage by 8% points. Moreover, a larger num-

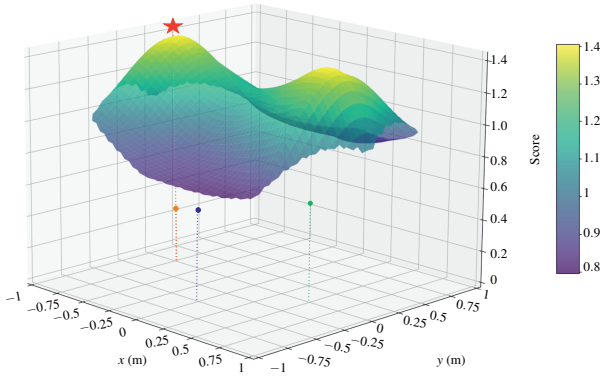

(a) Scenario 1 - $z = 0.4$

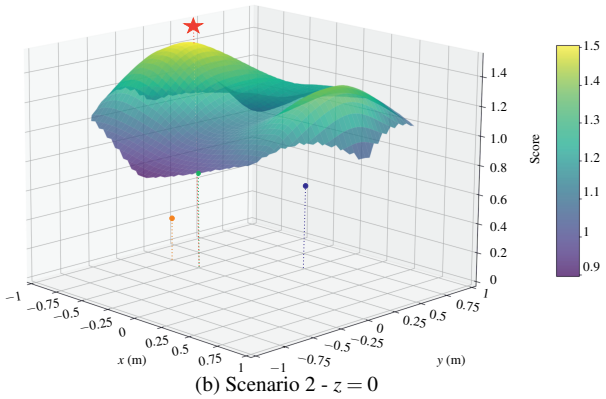

(b) Scenario 2 - $z = 0$

Figure 6: Score distribution across the two different scenarios. The two surfaces are obtained through interpolation of discrete data points (i.e., the score). The first row illustrates the score distribution for Scenario 1 when $z = 0.4$. The second row presents the score behavior for Scenario 2 with $z = 0$. The red star indicates the total maximum score for each scenario. The green, blue, and orange circles represent the maximum value of inspection pose feasibility ($F = F_1$ in (8)), pose distribution sparsity ($F = F_2$ in (8)), and inverse kinematic solution availability ($F = F_3$ in (8)), where each value is normalized between 0 and 1. Note that due to interpolation, the actual maximum values from the raw data (1.42 for Scenario 1 and 1.52 for Scenario 2) is not visualized precisely on the plots.

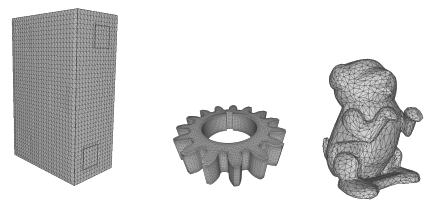

(a) Parallelepiped (b) Gear (c) Dog

Figure 7: 3D meshes of the inspected objects.

ber of feasible inspection poses corresponds to the possibility of finding more suitable inspection paths, determining, on average, a shorter inspection time.

Table 1: Performance metrics

Position	Object	Scenario	%	#FIPs	s
1	Parallelepiped	1	48	28	1
2	Parallelepiped	1	44	17	0.7
3	Parallelepiped	2	**65**	23	**0.5**
2	Parallelepiped	2	54	29	0.8
1	Gear	1	92	29	0.8
2	Gear	1	63	15	0.8
3	Gear	2	**96**	28	**0.8**
2	Gear	2	75	24	0.9
1	Dog	1	97	23	0.6
2	Dog	1	84	14	0.9
3	Dog	2	**100**	31	**0.2**
2	Dog	2	85	22	0.5

Position 1 is $(-0.75, 0, 0.4)$, Position 2 is $(0.75, -0.75, 0)$, and Position 3 is $(-0.5, 0, 0)$.

Outlook

In this work, we present a method for optimizing the placement of a robotic arm within a constrained inspection cell. Our approach addresses the challenges of designing a flexible robotic inspection system capable of handling objects with varying geometries and sizes without requiring reconfiguration. We employ an offline planning strategy to enable fast and efficient online inspections with high coverage.

The problem was formulated as an optimization task to determine the optimal robot base placement, considering constraints such as joint limits, collision avoidance, workspace boundaries, and camera-object line-of-sight occlusions. We introduced a novel cost function that balances inspection pose feasibility, pose distribution sparsity, and inverse kinematic solution availability. Bayesian optimization proved effective in solving the problem, showcasing its ability to handle high-dimensional optimization problems with costly evaluations.

The results underline the critical role of strategic robot placement in maximizing inspection coverage and minimizing inspection time. This methodology is particularly promising for flexible manufacturing environments, where adaptability and efficiency are paramount. By optimizing robot placement, the proposed approach reduces setup time, increases coverage, and enhances overall system performance.

Future directions include incorporating multi-robot setups to further enhance the flexibility and scalability of robotic inspection systems.

References

[1] T. Yoshikawa, "Manipulability and redundancy control of robotic mechanisms," in *IEEE International Conference on Robotics and Automation (ICRA)*, vol. 2, 1985, pp. 1004–1009.

[2] M.-J. Tsai, "Workspace geometric characterization and manipulability of industrial robots (kinematics)," Ph.D. dissertation, The Ohio State University, 1986.

[3] M. Sereinig, P. Manzl, and J. Gerstmayr, "Task dependent

comfort zone, a base placement strategy for mobile manipulators based on maniuplability measures," *Robotics*, vol. 13, no. 8, 2024.
[4] K. Abdel-Malek, W. Yu, and J. Yang, "Placement of robot manipulators to maximize dexterity," *International Journal of Robotics and Automation*, vol. 19, no. 1, pp. 6–14, 2004.
[5] B. Kamrani, V. Berbyuk, D. Wäppling, U. Stickelmann, and X. Feng, "Optimal robot placement using response surface method," *The International Journal of Advanced Manufacturing Technology*, vol. 44, pp. 201–210, 2009.
[6] K. Baizid, A. Yousnadj, A. Meddahi, R. Chellali, and J. Iqbal, "Time scheduling and optimization of industrial robotized tasks based on genetic algorithms," *Robotics and Computer-Integrated Manufacturing*, vol. 34, pp. 140–150, 2015.
[7] D. Spensieri, J. S. Carlson, R. Bohlin, J. Kressin, and J. Shi, "Optimal robot placement for tasks execution," *Procedia CIRP*, vol. 44, pp. 395–400, 2016.
[8] A. Wachter, C. Hartl-Nesic, and A. Kugi, "Robot base placement optimization for pick-and-place sequences in industrial environments," *IFAC-PapersOnLine*, vol. 58, no. 19, pp. 19–24, 2024.
[9] T. Bachmann, K. Nottensteiner, and M. A. Roa, "Automated planning of workcell layouts considering task sequences," in *IEEE International Conference on Robotics and Automation (ICRA)*, 2021, pp. 12 662–12 668.
[10] V. Staderini, T. Glück, P. Schneider, R. Mecca, and A. Kugi, "Surface sampling for optimal viewpoint generation," in *IEEE 13th International Conference on Pattern Recognition Systems (ICPRS)*, 2023, pp. 1–7.
[11] B. Shahriari, K. Swersky, Z. Wang, R. P. Adams, and N. De Freitas, "Taking the human out of the loop: A review of bayesian optimization," *Proceedings of the IEEE*, vol. 104, no. 1, pp. 148–175, 2015.
[12] A. Agnihotri and N. Batra, "Exploring bayesian optimization," *Distill*, 2020, access January 7, 2025. [Online]. Available: https://distill.pub/2020/bayesian-optimization
[13] J. Villalobos, I. Y. Sanchez, and F. Martell, "Statistical comparison of denavit-hartenberg based inverse kinematic solutions of the ur5 robotic manipulator," in *International Conference on Electrical, Computer, Communications and Mechatronics Engineering (ICECCME)*, 2021, pp. 1–6.
[14] L. Downs, A. Francis, N. Koenig, B. Kinman, R. Hickman, K. Reymann, T. B. McHugh, and V. Vanhoucke, "Google scanned objects: A high-quality dataset of 3d scanned household items," in *IEEE International Conference on Robotics and Automation (ICRA)*, 2022, pp. 2553–2560.

Author Biography

VANESSA STADERINI received her M.Sc. degree (cum laude) in robotics and automation engineering at the University of Pisa, Italy, in 2021. She is currently pursuing a PhD at the Faculty of Electrical Engineering and Information Technology at TU Wien, Vienna, Austria. She works on the development of inspection planning solutions for industrial applications at the Center for Vision, Automation & Control of the AIT Austrian Institute of Technology GmbH. Her research interests include robotics and computer vision for automotive and industrial applications.

TOBIAS GLÜCK (Member, IEEE) received a Dipl.-Ing. degree in technical cybernetics from the University of Stuttgart, Germany, in 2007, and the Ph.D. degree from TU Wien, Vienna, Austria, in 2013. He is currently with the AIT Austrian Institute of Technology GmbH, Vienna. His work focuses on thinking in systems and the holistic view of automation components and production processes. He develops and implements methods, algorithms, and technologies to optimize and control these complex dynamical systems.

ANDREAS KUGI (Senior Member, IEEE) received a Dipl.-Ing. degree in electrical engineering from TU Graz, Austria, in 1992, and a Ph.D. degree in control engineering and a habilitation degree in automatic control and control theory from Johannes Kepler University (JKU), Linz, Austria, in 1995 and 2000, respectively. He was an Associate Professor with JKU from 2000 to 2002 and a Full Professor with Saarland University, Saarbrücken, Germany, from 2002 to 2007. Since 2007, he has been a Full Professor of complex dynamical systems at the Automation and Control Institute, TU Wien, Vienna, Austria. From 2017 to 2023, he was the Head of the Center for Vision, Automation, and Control, AIT Austrian Institute of Technology GmbH, Vienna, where since July 2023, he has been the Scientific Director. His main research interests include modeling, nonlinear control and optimization of complex dynamical systems, mechatronic system design, robotics, and process automation. He is a Full Member of the Austrian Academy of Sciences and a Member of the German National Academy of Science and Engineering (acatech).